

Automatic Crack Detection and Quantification for Tunnel Lining Surface from 3D Terrestrial LiDAR Data

Hong Zhou *, Binwei Gao** and Wenjin Wu **

** Xiamen Engineering Technology Center for Intelligent Maintenance of Infrastructures, School of Architecture and Civil Engineering, Xiamen University, Room 506, Zeng Chengkui Building, No.182, Daxue Road, Siming District, Xiamen, Fujian, China. Email: mcwangzh@xmu.edu.cn*

*** Graduate student, Department of Civil Engineering, School of Architecture and Civil Engineering, Xiamen University, China*

**Corresponding Author: mcwangzh@xmu.edu.cn*

Submitted : 05-07-2022

Revised : 30-08-2022

Accepted : 04-09-2022

ABSTRACT

The rapid development of tunnel engineering has resulted in good safety management of tunnels becoming a research hotspot. The accurate detection of cracks is a major factor affecting the safety of tunnels, and thus has garnered the attention of scholars. The traditional crack detection method is manual photography and field recording, which is time-consuming and laborious. Thus, an automated and efficient crack detection method must be developed. In recent years, laser scanning has been used in road crack detection. Consequently, its introduction into tunnel engineering in terms of collecting three-dimensional point cloud from the tunnel, and subsequently detecting cracks is of significance. Therefore, this study proposed an automatic crack detection method, which can automatically identify the cracks from the tunnel three-dimensional point cloud and extract the crack information. This method combined the RANSAC and LMS algorithms to fit the point cloud surface data, and then expanded the cylinder. Further, the improved Alpha Shape algorithm based on Delaunay triangulation was used to extract the crack contour. Consequently, the limitation of using a single algorithm for crack extraction was improved in the proposed method. Further, the method was applied to the 36 m long lining experimental section of the Xiamen Metro Line 3 tunnel and the cracks extraction results were compared with those of the traditional manual visual inspection. The experimental results exhibited that more than 90% of the target registration accuracy of this method reached 0.001 m and below. Moreover, the maximum error of crack width extraction was only 0.20 mm, with relative error of width and length being less than 8%. Thus, the results confirmed the suitability of the proposed method for both straight and curved tunnels and its ability to automatically identify serious crack disease information efficiently and effectively.

Keywords: 3D LiDAR; Point Clouds; Tunnel Lining Surface; Crack Detection

INTRODUCTION

By December 2018, the operating mileage of urban rail transit in China reached 5494.9 km. Further, the urban rail transit engineering has changed from the stage of “large scale construction” to the stage of “equal emphasis between construction and maintenance” (Zhao & GU, 2019). However, tunnel engineering safety accidents have been occurring more frequently. Tunnel lining crack is a common disease that endangers structural safety, and thus rapid acquisition and efficient management of tunnel structural surface cracks are significantly crucial to the inspection, maintenance, and safety evaluation of the engineering structure (Yin et al., 2014).

The current practices for the crack detection of the main structure in the tunnel construction and operation are primarily reliant on field records and photographic surveys (Liu et al., 2017), which are time-consuming, labor-intensive, provide low data quality, and are unable to quantitatively provide the essential geometric information regarding the cracks (Huang et al., 2012). In the operation stage of subway tunnel engineering, the collection time of regular monitoring data is typically only allowed to complete data collection of more than 10 km within a few hours when the train is closed at night. This necessitates very high efficiency and quality of data collection. Thus, these limitations of the current practice render satisfying the requirements of the tunnel construction and its quarterly maintenance inspections challenging (Zhang et al., 2014).

With the development of science and technology, traditional two-dimensional detection technology are unable to satisfy the requirements of automatic and intelligent detection. Consequently, three-dimensional (3D) intelligent detection technology has attracted increasing attention. 3D laser scanning, referred to as “High-Definition Surveying (HDS)”, is a specific form of machine vision (Luh et al., 2013). Kattan et al., (2021) created a virtual 3-D model of the college of engineering/University of Duhok, Kurdistan Region, Iraq. Bhatti et al., (2021) scanned a 4-story public building using a 3D laser scanner to determine the architectural and structural drawings of the response to an earthquake. Zhu et al. (2010) used a MAGER 5006i fixed 3D laser scanner to scan the circumferential cracks in the Longxi Water supply Tunnel. Yin et al. (2014) measured the cracks in the 3D point cloud data collected by the Leica HDS6000 fixed 3D laser scanner. Compared with the conventional manual acquisition method, the advantages of automation, rapidness, and large-scale application of 3D laser scanning technology facilitate the exploration of more efficient detection methods of tunnel lining surface crack information. In recent years, 3D laser scanning technology has been used in the deformation monitoring of a certain major tunnel projects in the world. The advantages of employing a static LiDAR system for geotechnical and operational applications were demonstrated at a drill and blast tunnel operation at the Sandvika-Asker Railway Project near Oslo, Norway and in two other test tunnels (Fekete et al., 2010). Gikas, (2012) discussed the use and exploration potential of laser scanning technology to realize accurate tracking of excavation and construction activities of Athens suburban railway system in Greece. Moisan et al., (2015) realized the construction of a full 3D model of a canal tunnel in France through the combination of terrestrial laser and sonar scans collected from static acquisitions. Saydam et al., (2021) proposed a practical algorithm, CFBolt, to detect rock bolts from a 3D laser scanned point cloud, and was tested for detecting rock bolts from LiDAR scan data collected from Sydney’s civil tunnelling project site.

However, there are many aspects of tunnel detection, such as optimization of the 3D scanning technology and its better application and promotion in all aspects of tunnel engineering requires further research. Considering the above safety requirements of tunnel construction and operation, this study proposed a new tunnel lining crack detection method based on 3D scanning technology in an attempt to ensure better safety of tunnel engineering.

LITERATURE REVIEW

Current studies have developed efficient and reliable algorithms to realize the automation detection of bridges (Trias et al., 2022). Based on D-S theory, Huang et al. (2014) used the pavement crack detection, Random Sample Consensus (RANSAC) algorithm, point cloud coordinates information, and Alpha Shape algorithm to extract the crack outline. The experimental results showed that the method can identify the cracks on the rectangular wood beam and column surface. However, the Alpha Shape algorithm is inefficient and has obvious limitations when handling a multitude of engineering point clouds (Cabaleiro et al., 2017). In the studies based on the Delaunay triangulation network (Li et al., 2011), the defective and normal pavements were distinguished according to the geometric characteristics between the triangular surface of the pavement defect area and the normal triangular surface. Sun (2018) used the Least Mean Square (LMS) algorithm to fit the cross-section line of the road point cloud and consequently determine the position of the crack by fitting the wave valley of the curve. However, owing to the interference of pavement noise on the LMS algorithm as in Xu et al. (2014), the estimation results of the crack range were not accurate. Although in fields other than tunnel engineering, the crack detection algorithm based on 3D laser scanning technology has been studied to a certain extent, each algorithm still has its limitations.

Currently, research on the automation of 3D laser scanning technology in tunnel engineering is not yet mature. Point clouds do not overlap in many cases (Moisan et al., 2015), implying that the point cloud data for tunnel lining surface crack recognition is still manual (Truong-Hong & Laefer, 2014). Further, research on 3D laser scanning technology algorithms in tunnel engineering is still limited. Considering that the reflection intensity of the point cloud in dry pavement crack was lower than that of the surrounding pavement owing to the distance and angle, (Yu et al., 2014) proposed an algorithm of extracting crack shape from the 3D point cloud. The extraction results facilitated the identification of the crack shape; however, the crack width, length, and other key geometric information could not be identified. In addition, research on surface fitting algorithms is yet to be explored. The tunnel lining surface is curved, and the geometric information cannot be directly measured from the collected point cloud. Consequently, current tunnel lining surface surveys are performed through the processing of two-dimensional (2D) images or 3D LiDAR point cloud (Qu et al., 2016) to detect the tunnel lining surface and extract useful information for tunnel lining surface crack and leakage by image processing and object recognition (Zhang et al., 2014). Compared with 2D photography technology, the point cloud data collected by 3D ground laser radar can provide more one-dimensional information in theory, which renders the disease characteristics obvious; however, the existing photogrammetry machines are bulky with most being only suitable for highway tunnel tests. In addition, the types of tunnels currently applicable to tunnel lining surface investigations are susceptible to natural conditions. For example, the tunnel crack is often accompanied by water seepage (Yang & Xu, 2021), the reflection intensity of the point cloud inside the crack is close to the reflection intensity of the surrounding water leakage area. Although cracks with water leakage may be detectable, in case of certain cracks closed by white precipitates of calcium carbonate, the extraction of the water leakage crack

based on the difference of the reflection intensity is challenging (Jiang et al., 2019; Xiong et al., 2020). Consequently, the identification of the surface cracks and other diseases under conditions with limited light sources support becomes difficult (Zhou, 2017). This situation can be effectively improved if the light source conditions are satisfied. Therefore, the study of automatic detection technology in tunnels is still worthy of attention.

In summary, although many researchers have studied the deformation information of the tunnel main structure such as section deformation, clearance convergence, and ellipticity with the 3D point cloud data (Cheng, 2015), automation research related to cracks (Yin et al., 2014), structural damage, and leakage is still insufficient (Armesto-Gonzalez et al., 2010; Wu & Huang, 2018). outstudies in recent years have mainly focused on the crack identification and quantitative extraction of main geometric information, with most focused on highway pavement crack detection. Thus, there is an urgent need for a new method for automatic identification of tunnel lining surface cracks and quantitative estimation of crack size from point cloud data. Therefore, considering the limitations of the above algorithms, this study proposed an automatic detection and quantification method of tunnel lining surface cracks using 3D laser radar point cloud data. In the proposed method, first, to the method to properly collect the 3D point cloud data inside a tunnel to ensure data quality and robustness was introduced. Subsequently, the collected raw data was prepared through pre-processing. Finally, a method of automatically identifying cracks based on the pre-processed tunnel lining surface point cloud was proposed and the crack geometry information was estimated.

METHODOLOGY

This study proposed an automatic tunnel lining surface crack detection method to identify the cracks from 3D terrestrial LiDAR data and quantify the size of the identified cracks. The main research framework is shown in Fig. 1. The proposed methodology has three major steps: 1) data collection, 2) data pre-processing, and 3) automatic crack detection and quantification. To provide a good quality of data for the third step, we must start with an accurate and detailed planned data collection and pre-processing process. We established a point cloud acquisition scheme through a systematic analysis of the relationship between crack detection accuracy and scanner parameters, station spacing, and tunnel geometry. With the collected and pre-processed data from steps 1 and 2, we integrated the RANSAC, LMS, and Alpha Shape algorithms to remove outliers and noise, fit the surface model, and finally detect crack outlines. This Section explains the principle of the method used.

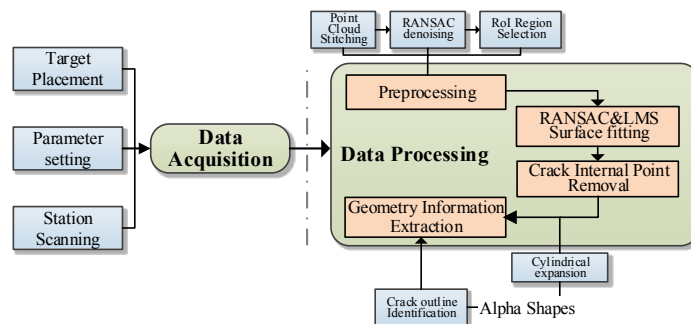


Fig. 1 Framework of the Proposed Research Methodology

Data Collection

A tunnel is an ultra-long linear structure, and point cloud data collection inside the tunnel is encounters challenges owing to the scanning angle of view, scanning distance, and scanning accuracy of the 3D terrestrial laser scanner. Therefore, the entire tunnel must be divided into several scanning stations along the tunnel axis, and targets were used during the data collection for registering all the scans. The key aspects of data collection were the setting of station spacing, scanning resolution, and target placement, which affect the accuracy and efficiency of the 3D point cloud data collection process. The station spacing was set according to the inner diameter of the tunnel and the maximum incident angle of laser reasonably (Wang et al., 2013). As shown in Fig.2(a), each scanning station was set up at the central axis of the tunnel. For station 2, the measuring point with the maximum incident Angle was located at endpoint B. The maximum incident angle θ_{max} of the laser within the scanning range of station 2 can be calculated as follows:

$$\theta_{max} = \arctan \frac{S}{D} \quad (1)$$

where S is the station spacing (m) and D is the inner diameter of the tunnel (m). For the relationship between S and D, considering the complex ground environment in the tunnel construction site, and other factors, it is difficult for the center of the scanner to locate on the axis of the tunnel center. Based on the findings from a recent study (Tang et al., 2007), we considered $S = (1 - 2)D$.

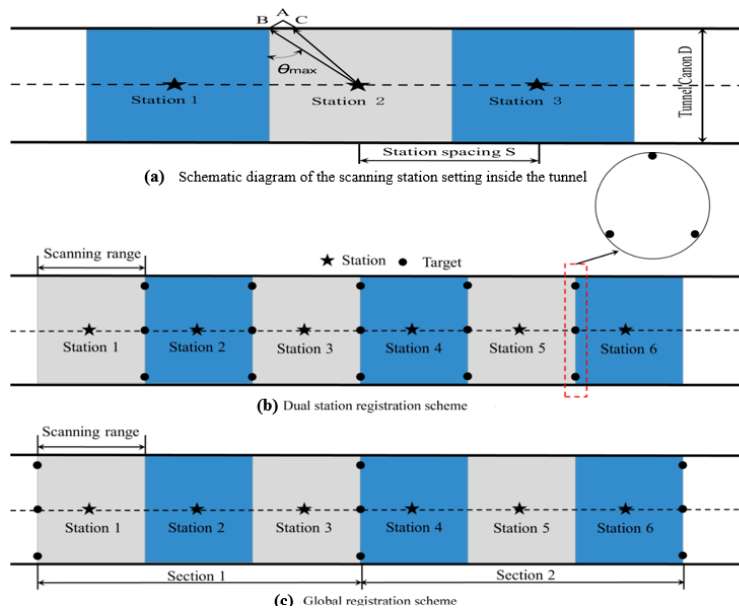


Fig. 2. Schematic of station setting and registration scheme

Figure 2(b) is a commonly used bistatic registration method, wherein the targets are arranged in the connecting part between two adjacent stations. At the time of registration, one scanning station is selected as the reference station, and the other stations are registered with the adjacent previous stations respectively. However, with

the increased times of registration needed, the registered data of the long-narrow tunnel structure may experience serious deformation. Consequently, Kang et al. (2013) proposed a global registration method to divide the tunnel into different sections, where each section contained a number of stations, and the targets arranged at both ends of the section were used as the common registration control point for each station in the corresponding section. Further, Becerik-Gerber et al., (2011) found that the measurement error of the target was independent of the measurement distance. Therefore, it is evident that the length of the section can be determined based on the ground environment, visual conditions, required point cloud density, scanner parameters, and other factors. In the global registration method shown in Fig.2(c), every three stations are together defined as a section, and three stations in one section are registered in the same coordinate system with common control points. The point cloud data of the three stations in the section is integrally controlled. With reduction in the incident angle from the laser to the center of the target, it is more beneficial to accurately obtain the coordinates of the center of the target and thus reduce the point error of the control points. This could reduce the number of control points, thereby reducing the cost of labor and material costs in the data collection process and improving data collection efficiency.

Data Pre-Processing

The purpose of point cloud data pre-processing was to prepare the collected point cloud data and render them ready for the later step - tunnel crack detection. This study processed the collected data in Cyclone 9.0, using which, database creation and import, point cloud registration, point cloud de-noising, and Region of Interest (RoI) extraction operations may be performed. At the end of pre-processing, a text file (.txt format) is generated for the next step.

Point Cloud Registration

Unifying the point clouds of different sites into the same coordinate system is referred to as point cloud registration (Becerik-Gerber et al., 2011). Rigid body transformation such as translation and rotation is performed in the point cloud registration without distortion and scaling. The method of point cloud registration can be mainly categorized into three groups: target-based, targetless based, and mixed stitching. Because the tunnel structure is linearly narrow, there are no obvious characteristic points in the point cloud data. Thus, to ensure the efficiency and accuracy of registration, target-based registration was adopted in this research.

Point Cloud De-noising

The original point cloud contains considerable noise data. For mixed points, the RANSAC algorithm is used to eliminate point cloud noise in surface fitting and then the optimal model is fitted to obtain the effective local point set after eliminating the influence of external points. Finally, the LMS algorithm is used to fit the effective local point set.

RoI Region Selection

Next, to avoid the high computational complexity of global surface fitting of tunnel point cloud (Chen, 2016) and effectively reduce the computing calculation cost and improve the accuracy of surface fitting in the local area where the crack is located, local surface fitting to the RoI where the crack is located was adopted (Cabaleiro et al., 2017). Following the selection of the RoI areas, we converted the point cloud in the RoI area to a text format file, which can be analyzed using the proposed tunnel detection algorithm for further data processing.

Crack Detection from Point Cloud

Surface fitting of point cloud data

In this step, we integrated the RANSAC and LMS algorithms to fit the point cloud surface data, which is more robust and accurate than the traditional fitting method (Wei & Liu, 2014). First, the RANSAC algorithm was used for the sampling iterative fitting to obtain the best estimation model and the effective local point set corresponding to the model. In this process, data de-noising and outliers removal were performed. Subsequently, the LMS algorithm was introduced to fit the effective local point set of the best estimation model, such that the algorithm is not affected by the external points and the points with large errors in the data. Moreover, this ensures that the fitting model closest to the ideal model was obtained. The flow chart of the algorithm is shown in Fig. 3.

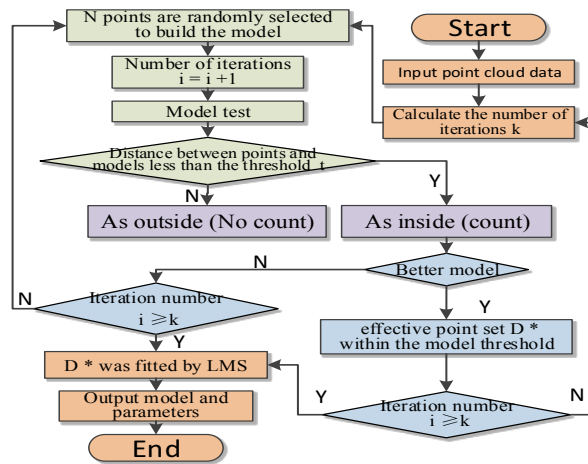


Fig. 3. Flowchart of surface fitting method combined with RANSAC algorithm

This study used the LMS algorithm for the optimal model. At this time, the observed data were no longer the original sample data, instead, the data after eliminating certain local points by the RANSAC algorithm were considered. The process reduced the external points and noise in the data and improved the accuracy and rationality of the fitting results greatly.

Crack point clouds removal and extract

Following the curve fitting of the point cloud on the lining surface, the point cloud collected in the crack still exists, which affects the geometry extraction of the subsequent cracks. Therefore, the point cloud inside the crack must be removed. Following the removal, the point cloud was projected and expanded onto the fitting surface, and the 3D point cloud was then transformed into a 2D plane. Figure 4 shows the removal process of the point cloud inside the crack. Here, L is a critical value defined by the 3D LiDAR scan parameters, as shown in Eq. 2 (Cabaleiro et al., 2017):

$$L = \sigma \alpha_c \quad (2)$$

where σ is the accuracy of 3D LiDAR and α_c is the range value obtained through multiple tests.

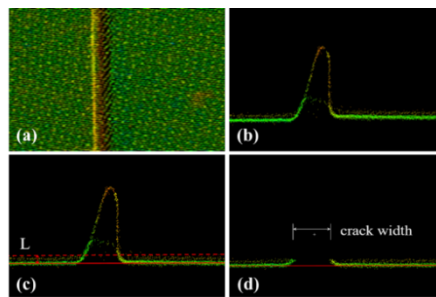


Fig. 4. Point cloud removal process inside the crack. (a) Front view of crack point cloud; (b) Side view of the fracture point; (c) Remove points beyond the critical value; (d) Side view after the removal

Following the removal of the crack point cloud, the cylindrical surface was projected and expanded to a planar surface. The principle of point cloud projection and expansion is shown in Fig. 5(a). With cylindrical section fitting center $O(x_0, z_0)$ as the center, the projection of all points to the algorithm fit surface is shown by the solid line in Fig. 6. The projection result was expanded along the top of the fitting surface, and the 3D point cloud was converted to a 2D plane. In Fig.5, $P = (x, z)$ is a point in the point cloud, $P' = (x', z')$ is the point projected by P , and $P'' = (x'', z'')$ is the point after P' is expanded along the top of the fitting cylinder. Further, $OA = (1, 0)$ is the positive X-axis unit vector, and $OB = (0, 1)$ is the positive z-axis unit vector.

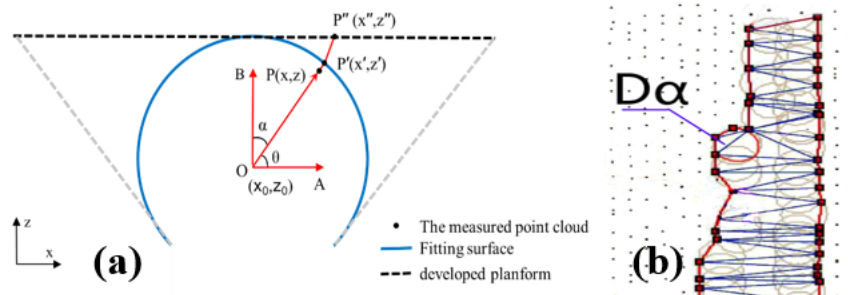


Fig. 5. (a) Point cloud projection and expansion diagram Crack outline recognition and geometry extraction

(b) The diameter of the circumferential circle and its geometric outline formed by edge points (Cabaleiro et al., 2017)

Following the cylinder expansion, we used the improved Alpha Shape algorithm based on Delaunay triangulation to extract the outline of the crack. The algorithm first performed an incremental insertion method to construct the Delaunay triangulation network and then examined whether each edge of the triangulation network conformed to the conditions of Alpha Shape in turn. Following the coordination of the circle center with the outer circle diameter, $D\alpha$ of the edge was calculated according to the Distance Intersection Method (DIM) (Cabaleiro et al., 2017), which measures the distance from the remaining points to the center of the circle. If the measured distance was greater than $D\alpha/2$ (the radius), the circumscribed circle did not contain the remaining points, and the edge was the Alpha Shape edge. All Alpha Shape edges satisfying the requirements constituted the outlines of the crack. As shown in Fig.5(b), the area recognized by Alpha Shape was the sum of the area of all triangles.

FIELD EXPERIMENT AND RESULTS

Point Cloud Data Collection

Wujanz et al., (2017) exclusively investigated the phase-based range finder, Riegl VZ-400i pulse scanner, and Leica scanning station P40 using hybrid ranging strategy. Research showed that as the stochastic characteristics of these laser scanners can also be described by intensity-based stochastic models, their generality was assured. The parameters of Leica P40 3D laser scanner were as follows: range accuracy: 1.2 mm + 10 ppm, angle accuracy: Angle accuracy 8"/8" (vertical/horizontal), range noise: noise accuracy 0.4 mm @10 m, and target acquisition accuracy: 2 mm (Wujanz et al., 2018). With horizontal and vertical resolutions of 2 mm each for a distance of 2 m (Piech et al., 2018), Leica P40 was considered suitable for this case study. Based on the above research, to validate the feasibility of the proposed methodology, we used a Leica P40 3D laser scanner to scan a section of Xiamen Metro Line 3.

The inner diameter and width of the measured tunnel segment were 5.5 and 1.2 m, respectively. For this experiment, we selected a section of the tunnel measuring 36 m as the testing object and used MATLAB to implement the proposed methodology. The 3D model for analyzing the diagram of segment lining is shown in Fig. 6.

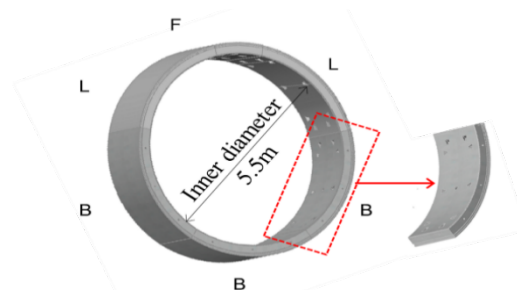


Fig. 6. 3D model of tunnel lining

Because the inner diameter of the tunnel was $D=5.5\text{ m}$, according to the calculation method of station spacing in Section 3.1. in the data collection process, the distance between two stations was set as $S = 6\text{ m}$, that is, the width of 5 segments. To arrange the location of the targets for the registration, we divided the 36 m long testing section into two isometric sections. Each section was then further divided into three scanning stations and had three targets set at both ends of the section as the common registration control points. Two targets were used at the junction of the two sections as the registration control points of the two sections. The detailed layout of the scanning station, target location, and registration scheme is shown in Fig. 7, following consideration on easily setting up the target and satisfying the requirement of no less than two targets between every two adjacent scans. Figure 8 shows the Leica P40 and two targets in the tested tunnel.

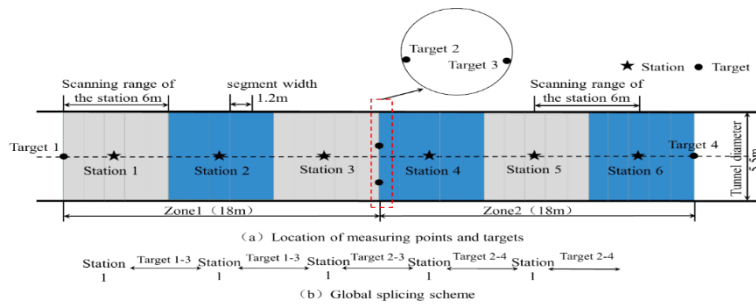


Fig. 7 The station, target layout and splicing scheme



Fig. 8. On-site data acquisition

Results and analysis of the preprocessing of the testing point cloud data

In the experiment, we pre-processed the collected point cloud data in Cyclone 9.0. Through the establishment and improvement of the database described in Section 3.2, point cloud registration, point cloud denoising, and ROI area extraction were performed in that order. The pre-processing results are shown in Fig. 9. Finally, the pre-processed data was exported as a text file for crack detection in the next step.

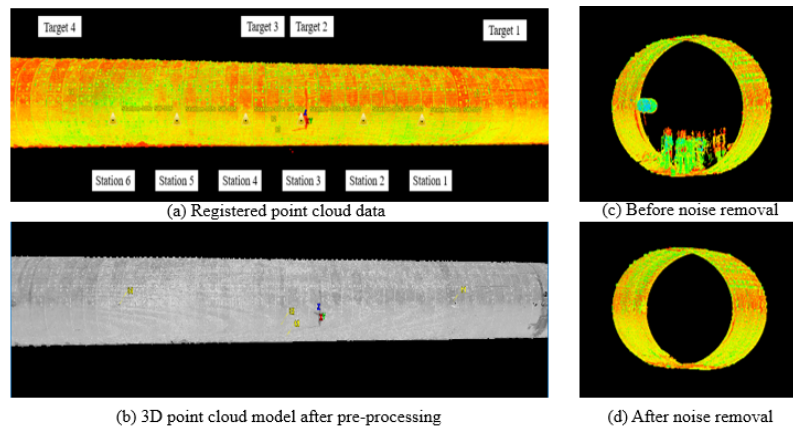




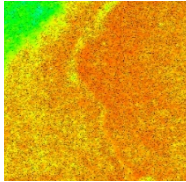
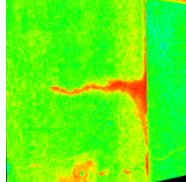
Fig.9 Point cloud pre-processing process

The analysis results of the pre-processing indicated that more than 90% of the target registration reached an accuracy of 0.001 m or less, with the rest being 0.002 m, which satisfied the requirements of registration accuracy as

a whole. The registration accuracy of 0.002 m appeared at both ends of the section because only one target was provided at both ends of the section. Therefore, for future experiments, the number of targets at both ends of the section should be set to two or three to control the overall registration accuracy.

In the experiment, we manually selected three different cracks with good quality for the crack detection accuracy analysis. Among the three cracks, the length of Crack 1 was small with large width, the length of Crack 2 was larger with a small width, and Crack 3 was small and of an irregular shape. Cracks 1 and 2 were also accompanied by obvious water leakages, and the reflection intensity of the collected point cloud was higher in the leakage area. The crack detection results of the RoI region are presented in Table 1. Exporting the “x, y, z,” the 3D coordinates of each crack RoI were exported and converted into a text format.

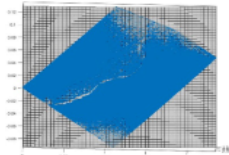

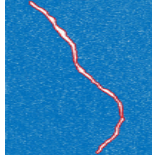
Table 1. Crack RoI region extraction

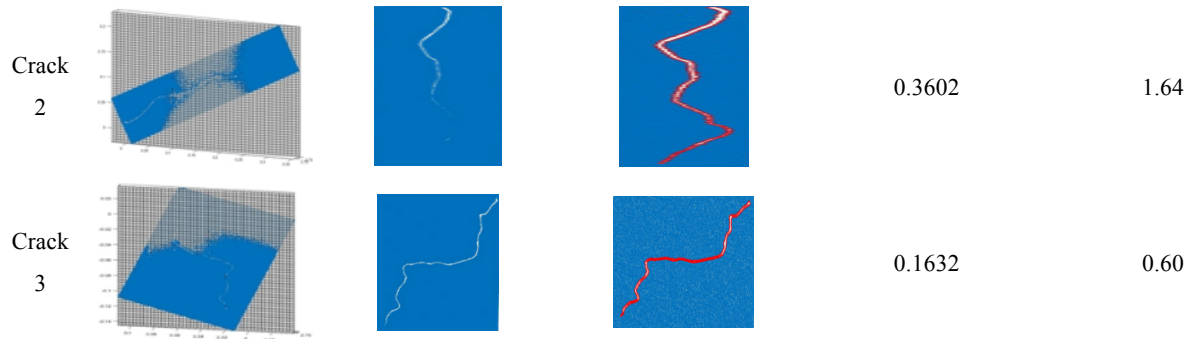
No	1	2
Picture		
RoI		

Results and analysis of the tunnel crack detection and quantification

The experiment continued with processing the preprocessed point cloud data from the previous step. The surface fitting algorithm by integrating the RANSAC and LMS algorithms was used to fit the surface of the RoI region. The absolute fitting errors were estimated as 6.59×10^{-4} , 1.50×10^{-3} , and 6.90×10^{-4} and were dimensionless. According to Eq. (2), the points beyond the distance $L=0.002$ m of the fitting surface were considered as the internal point of the crack and removed. Further, the surface expansion diagram of the remaining points was projected to the fitting surface. The results of the crack surface fitting and cloud projection expansion are presented in Table 2.

Table 2. Results of crack surface fitting, projection expansion and extraction

NO.	Fitting surface	expansion Dwg	Extracted crack outlines	Length (m)	Maximum Width (mm)
Crack 1				0.1527	5.52



Thereafter, we continued to extract the crack geometry information by using the improved Alpha Shape algorithm based on the Delaunay triangulation method. The minimum area value was set as $A_{min}=5.0\times 10^{-5} \text{ m}^2$. The extraction results of crack outline and geometric information are summarized in Table 2. Subsequently, we analyzed the crack detection accuracy through comparisons of the extracted crack length and width in the experiment with the manual close-distance measurement using a steel tape and crack width detector. The statistics and analysis of crack extraction accuracy are presented in Table 3.

Table 3. Statistics and analysis of crack extraction results

NO	Length			
	Extraction Results L1 (mm)	Measured Value L2 (mm)	Absolute Error (mm) $S= L1-L2 $	Relative Error (%) $S/L2$
1	152.7	161	8.3	5.16
2	360.2	398	37.8	9.50
3	163.2	176	12.8	7.27
Average	—	—	19.63	7.31
Maximum Width				
1	5.52	5.72	0.20	3.50
2	1.64	1.77	0.13	7.34
3	0.60	0.64	0.04	6.25
Average	—	—	0.12	5.86

Table 3 indicates that the average relative error of the three sets of data was 7.31 % for the maximum length of the crack. Further, for the maximum crack width, the average relative error of the three sets of data was 5.86 %. Thus, the error range was within 8 %, which proves the feasibility of the method to a certain extent.


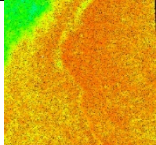

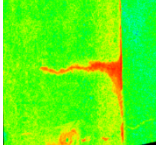

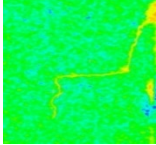

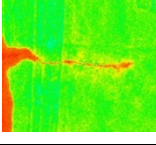
DISCUSSIONS


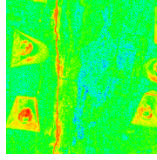

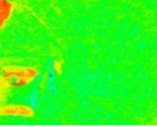
Considering all the results obtained from the experiment, we performed a statistical analysis of the 36 m long lining experimental section of the Xiamen Metro Line 3 tunnel and compared it with the traditional manual visual inspection statistical table of crack information. The comparison results are presented in Table 4. The results of the manual inspection could only provide the approximate location and the type of cracks. However, our proposed crack detection method offered the exact location mark of cracks in the tunnel and the estimated value of the crack length and width through the detection with a relative error within 8%, which is within the commonly acceptable error range by the inspection professionals. Crack No. 6 could recognize the corresponding geometric information because the its width was less than the acquisition accuracy.

According to the comparison and analysis of the crack geometric information extracted based on our proposed method with the manual inspection results, it is evident that:

(a) Although the relevant geometric information could not be extracted for the microcracks owing to various factors, it still satisfied the requirements of the current relevant regulations in countries. The conventional manual visual inspection method adopted by the stakeholders can only record an image of the identified lining crack and a description of the corresponding crack without specific dimension information.

Table 4. Comparison between manual crack inspection and automatic crack detection from point cloud

Manual Visual Inspection				Automatic crack detection from 3D point cloud data				
NO.	Location	Crack Type	Inspection image	NO.	Location (m)	Width (mm)	Length (m)	RoI of Point Cloud
TYGP-011	16	Seepage Crack		1	3.7	5.52	0.1527	
TYGP-015	33	Seepage Crack		2	23.0	1.64	0.3602	
TYGP-012	19	Edge Crack		3	7.3	0.60	0.1632	
TYGP-013	26	Seepage Crack		4	16.5	3.05	0.7580	

TYGP-014	26	Long Cracks		5	16.0	3.47	0.8904	
TYGP-016	38	Microscopic cracks		6	31.0	<0.5	—	

(b) The maximum measuring point spacing in the cloud was $\delta_{\max} = 0.5mm$. In theory, this data collection scheme can obtain the crack information of tunnel lining surface for width larger than 0.5 mm. The experimental results show that the proposed algorithm can extract the crack width information with a minimum width of 0.6 mm, which is consistent with the theoretical analysis. According to the classification standard of the width of the cracks in the tunnel lining (Lai et al., 2015), crack widths larger than 0.5 mm are considered as Class A cracks, which indicates that it is a serious issue. The proposed method can extract the geometry information of the cracks with a serious status. Based on this extra information, the project manager can take proper repair and treatment actions for cracks of different widths, and thus provide specific data for the related grading evaluation of the influence of cracks on the construction quality and risk of the tunnel structure.

CONCLUSIONS

This study introduced a new method of crack detection of tunnel lining surface from 3D terrestrial laser scanner data. This method was applied to a lining experimental section of the Xiamen Metro Line 3 tunnel and the cracks extraction results were compared with the results of traditional manual visual inspection. The conclusions drawn were as follows:

- (1) The target-based registration adopted in this study can satisfy the registration efficiency and accuracy. We divided the testing section into two isometric sections. Each section comprised three targets set at both ends of the section as the common registration control points. Further, two targets were used at the junction of the two sections as the registration control points of the two sections. The analysis results of the pre-processing showed that more than 90% of the target registration reached an accuracy of 0.001 m or less, and the rest were 0.002 m, which satisfied the requirements of registration accuracy as a whole.
- (2) Within the allowable range of accuracy, this method was more efficient and time-saving than the manual detection method, and thus can replace the manual detection method to a certain extent. The comparison results with the manual detection method showed that the maximum error of crack width extraction was only 0.20 mm, and the relative errors of width and length were less than 8%.
- (3) The method proposed in this study is suitable for both straight and curved tunnels. This study was focused on curved cracks. Cylindrical projection was involved in the application process. As the straight tunnel does not need to undertake surface expansion, the straight tunnel crack is simpler and can also be detected by this method.

- (4) This method compensates for the limitation of using a single algorithm. The combination of the LMS, RANSAC, Alpha Shape, and Delaunay Triangulation algorithms improved the accuracy of crack extraction. The extracted data was no longer the original sample data, rather, it was the data optimized by the comprehensive algorithm.

The proposed method realizes automatic extraction of tunnel cracks. However, this method still has certain limitations. In the case study, we chose a conventional tunnel. The applicability of this method in tunnels with complex working conditions requires further research and improvement. In addition, in the process of selecting the seepage crack acquisition, the area with better light source contrast intensity was selected, and the extraction accuracy of the crack area with poor light source contrast requires optimization.

The crack detection method proposed in this study is primarily the automatic extraction of crack geometric information. Methods to comprehensively utilize the point cloud coordinate information, color information, and reflection intensity information of the target object obtained by the three-dimensional laser scanner under the consideration of the surrounding environment are certain future research direction. In addition, the existing scanning equipment is large in size. Thus, the application of the excellent technology of large equipment to miniaturized equipment for more portable tunnel crack scanning is a very innovative and meaningful research for the future.

ACKNOWLEDGMENTS

This research was supported by the National Natural Science Foundation of China (Grant No. 71871192), the China Railway South Investment Group Co. LTD, Major Science and Technology Planning 2016 “Xiamen Metro No. 3 Line Cross-sea Tunnel Construction Risk Integrated Control and System Development”, and “2017 Xiamen Construction Science and Technology Project (XJK2017-1-9)”.

REFERENCES

- Armesto-Gonzalez, J., Riveiro-Rodriguez, B., Gonzalez-Aguilera, D., & Rivas-Brea, M. T. (2010).** Terrestrial laser scanning intensity data applied to damage detection for historical buildings. *Journal of Archaeological Science*, 37(12), 3037-3047. <https://doi.org/10.1016/j.jas.2010.06.031>
- Becerik-Gerber, B., Jazizadeh, F., Kavulya, G., & Calis, G. (2011).** Assessment of target types and layouts in 3D laser scanning for registration accuracy. *Automation in Construction*, 20(5), 649-658. <https://doi.org/10.1016/j.autcon.2010.12.008>
- Bhatti, A. Q., Wahab, A., & Sindi, W. (2021).** Application of 3D Laser Scanning for Digitization, Design and Analysis of Multistoried Building. *Journal of Engineering Research*(Online First Articles). <https://doi.org/https://doi.org/10.36909/jer.13419>
- Cabaleiro, M., Lindenbergh, R., Gard, W. F., Arias, P., & van de Kuilen, J. W. G. (2017).** Algorithm for automatic detection and analysis of cracks in timber beams from LiDAR data. *Construction and Building Materials*, 130, 41-53. <https://doi.org/10.1016/j.conbuildmat.2016.11.032>
- Chen, M. (2016).** *Research on Mass Data Processing and Application of Laser Scanning in Subway Shield Tunnel* [Master, Beijing Jiaotong University]. <https://doi.org/10.7666/d.Y3124311>
- Cheng, Y. (2015).** *Research and design of tunnel lining crack detection system based on image processing* [master's degree, Taiyuan University of Technology]. <https://doi.org/10.7666/d.Y2797958>
- Fekete, S., Diederichs, M., & Lato, M. (2010).** Geotechnical and operational applications for 3-dimensional laser scanning in drill and blast tunnels. *Tunnelling and Underground Space Technology*, 25(5), 614-628. <https://doi.org/10.1016/j.tust.2010.04.008>
- Gikas, V. (2012).** Three-Dimensional Laser Scanning for Geometry Documentation and Construction Management of Highway Tunnels during Excavation. *Sensors*, 12(8), 11249-11270. <https://doi.org/10.3390/s120811249>
- Huang, J. P., Liu, W. Y., & Sun, X. M. (2014).** A Pavement Crack Detection Method Combining 2D with 3D Information Based on Dempster-Shafer Theory. *Computer-Aided Civil and Infrastructure Engineering*, 29(4), 299-313. <https://doi.org/10.1111/mice.12041>
- Huang, Y., Liu, X., Yuan, Y., Liu, C., & Wang, X. (2012).** Auto Inspection Technology for Detecting Leakage in a Shield Tunnel. *Journal of Shanghai Jiaotong University | J Shanghai Jiaotong Univ*, 46(01), 73-78. <https://doi.org/10.16183/j.cnki.jsjtu.2012.01.016>
- Jiang, D., Zhang, W., & Liu, Y. (2019).** Detection of tunnel cracks and seepage areas in multi-scale space. *Journal of Tongji University (Natural Science)*, 47(12), 1825-1830. <https://kns.cnki.net/kcms/detail/31.1267.N.20200107.1846.026.html>
- Kattan, R. A., Abdulrahman, F. H., Gilyana, S. M., & Zaia, Y. Y. (2021).** 3-D modelling and visualization of large building using photogrammetric approach. *Journal of Engineering Research*(Online First Articles). <https://doi.org/https://doi.org/10.36909/jer.12167>

- Kang, Z., Tuo, L., Wang, B., & Xie, Y. (2013).** *Subway Tunnel Deformation Monitoring Based on 3D Laser Scanning Data* [Master, China University of Geosciences]. <https://doi.org/10.19349/j.cnki.issn1006-7949.2013.05.024>
- Lai, J., Qiu, J., Pan, Y., Cao, X., & Fan, H. (2015).** Comprehensive monitoring and analysis of segment cracking in shield tunnels. *Modern Tunnelling Technology*, 52(2), 186-191. <https://doi.org/10.13807/j.cnki.mtt.2015.02.028>
- Li, Q., Zou, Q., & Liu, X. (2011).** Pavement Crack Classification via Spatial Distribution Features. *Eurasip Journal on Advances in Signal Processing*, Article 649675. <https://doi.org/10.1155/2011/649675>
- Liu, J., Li, H., Jiang, X., & Chang, H. (2017).** *Application of linear CCD in tunnel crack detection* (Vol. 10256). SPIE. <https://doi.org/10.1117/12.2257653>
- Moisan, E., Charbonnier, P., Foucher, P., Grussenmeyer, P., Guillemain, S., & Koehl, M. (2015).** Adjustment of Sonar and Laser Acquisition Data for Building the 3D Reference Model of a Canal Tunnel. *Sensors*, 15(12), 31180-31204. <https://doi.org/10.3390/s151229855>
- Moisan, E., Charbonnier, P., Foucher, P., Grussenmeyer, P., Guillemain, S., & Koehl, M. (2015).** Building A 3D Reference Model For Canal Tunnel Surveying Using Sonar And Laser Scanning. *Int. Arch. Photogramm. Remote Sens. Spatial Inf. Sci., XL-5/W5*, 153-159. <https://doi.org/10.5194/isprsarchives-XL-5-W5-153-2015>
- Ogura, K., Zhu, J., Tanaka, T., & Saito, Y. (2011, Nov 16-18).** Characteristics of Excimer Laser Ablation for Three Dimensional Machining of PMMA. *Key Engineering Materials* [Proceedings of precision engineering and nanotechnology (aspen2011)]. 4th International Conference of Asian-Society-for-Precision-Engineering-and-Nanotechnology (ASPEN 2011), Hong Kong Polytech Univ, Hong Kong, PEOPLES R CHINA. <https://doi.org/10.4028/www.scientific.net/KEM.516.192>
- Piech, I., Kwoczyńska, B., Slowik, D., & Ieee. (2018, Jun 21-23).** Using Terrestrial Laser Scanning in Documentation of Antique Vehicles. [2018 baltic geodetic congress (bgc-geomatics 2018)]. Baltic Geodetic Congress (BGC-Geomatics), Olsztyn, POLAND.
- Qu, Z., Bai, L., An, S. Q., Ju, F. R., & Liu, L. (2016).** Lining seam elimination algorithm and surface crack detection in concrete tunnel lining. *Journal of Electronic Imaging*, 25(6), Article 063004. <https://doi.org/10.1117/1.Jei.25.6.063004>
- Sun, D. (2018).** *Research on parallel algorithm and defect detection method of road point cloud modeling* [Master, Harbin Institute of Technology]. http://www.wanfangdata.com.cn/details/detail.do?_type=degree&id=D01586224
- Saydam, S., Liu, B., Li, B., Zhang, W., Singh, S. K., & Raval, S. (2021).** A Coarse-to-Fine Approach for Rock Bolt Detection From 3D Point Clouds. *Ieee Access*, 9, 148873-148883. <https://doi.org/10.1109/access.2021.3120207>
- Tang, P., Akinci, B., & Garrett, J. H. (2007, sept 19-21).** Laser Scanning for Bridge Inspection and Management. *Improving Infrastructure Worldwide IABSE Symposium: Improving Infrastructure Worldwide*, Weimar, Germany. <https://doi.org/10.2749/222137807796120283>
- Trias, A., Yu, Y., Gong, J., & Moon, F. L. (2022).** Supporting quantitative structural assessment of highway bridges through the use of LiDAR scanning. *Structure and Infrastructure Engineering*, 18(6), 824-835.

<https://doi.org/10.1080/15732479.2021.1880446>

- Truong-Hong, L., & Laefer, D. F. (2014).** Application of Terrestrial Laser Scanner in Bridge Inspection: Review and an Opportunity. Iabse Symposium Report, Madrid, Spain. <https://doi.org/10.19349/j.cnki.issn1006-7949.2013.05.024>
- Wang, L., Cheng, X., & Wan, C. (2013).** Research on tunnel detection technology based on 3D laser scanning technology. *Geotechnical Investigation & Surveying*, 41(07), 53-57. https://kns.cnki.net/kcms/detail/detail.aspx?dbcode=CJFD&dbname=CJFD2013&filename=GCKC201307011&uniplatform=NZKPT&v=KWTvbt47XIv0UeeIVSPmM5M_OgVJm3qbByZLRg0CnxvpowUBAoDDKvrx83VJKP
- Wei, Y., & Liu, X. (2014).** Robust Plane Fitting of Point Clouds Based on RANSAC. *Journal of Beijing University of Technology*, 40(03), 400-403. <https://kns.cnki.net/kcms/detail/detail.aspx?dbcode=CJFD&dbname=CJFD2014&filename=BJGD201403015&uniplatform=NZKPT&v=q3NZCh5mU3ZfUwrUgAZXxK9OHs8hwIVNq75inbSdpMXmpSQxCgRoqA8zK8Qsisy5>
- Wu, C., & Huang, Y. (2018).** Laser scanning inspection method and application for metro tunnel leakage. *Journal of Natural Disasters*, 27(04), 59-66. <https://doi.org/10.13577/j.jnd.2018.0408>
- Wujanz, D., Burger, M., Mettenleiter, M., & Neitzel, F. (2017).** An intensity-based stochastic model for terrestrial laser scanners. *ISPRS Journal of Photogrammetry and Remote Sensing*, 125, 146-155. <https://doi.org/https://doi.org/10.1016/j.isprsjprs.2016.12.006>
- Wujanz, D., Burger, M., Tschirschwitz, F., Nietzschmann, T., Neitzel, F., & Kersten, T. P. (2018).** Determination of Intensity-Based Stochastic Models for Terrestrial Laser Scanners Utilising 3D-Point Clouds. *Sensors*, 18(7), Article 2187. <https://doi.org/10.3390/s18072187>
- Xiong, L., Zhang, D., & Zhang, Y. (2020).** Water leakage image recognition of shield tunnel via learning deep feature representation. *Journal of Visual Communication and Image Representation*, 71, 102708. <https://doi.org/https://doi.org/10.1016/j.jvcir.2019.102708>
- Xu, D. J., Yin, B., Wang, W., & Zhu, W. (2014).** Variable Tap-Length LMS Algorithm Based on Adaptive Parameters for TDL Structure Adaption. *Ieee Signal Processing Letters*, 21(7), 809-813. <https://doi.org/10.1109/lsp.2014.2317752>
- Yang, H., & Xu, X. (2021).** Structure monitoring and deformation analysis of tunnel structure. *Composite Structures*, 276, Article 114565. <https://doi.org/10.1016/j.compstruct.2021.114565>
- Yin, H., Feng, Q., Liao, Z., Jiang, L., & Cai, J. (2014).** Disease Tunnel Monitoring Based on 3D Laser Scanning Technology. *Chinese Journal of Underground Space and Engineering | Chin J Undergr Space Eng*, 10(4), 895-901.
- Yu, Y. T., Li, J., Guan, H. Y., Wang, C., & Ieee. (2014, Jul 13-18).** 3D Crack Skeleton Extraction from Mobile LiDAR Point Clouds. *IEEE International Symposium on Geoscience and Remote Sensing IGARSS [2014 ieee international geoscience and remote sensing symposium (igarss)]*. IEEE Joint International Geoscience and Remote Sensing Symposium (IGARSS) / 35th Canadian Symposium on Remote Sensing, Quebec City, CANADA.

- Zhang, W., Zhang, Z., Qi, D., & Liu, Y. (2014).** Automatic Crack Detection and Classification Method for Subway Tunnel Safety Monitoring. *Sensors*, *14*(10), 19307-19328. <https://doi.org/10.3390/s141019307>
- Zhao, X., & GU, B. (2019).** Statistical Analysis of Urban Rail Transit Lines in 2018 China. *Urban Mass Transit | Urban Mass Trans*, *22*(01), 1-7. <https://doi.org/10.16037/j.1007-869x.2019.01.001>
- Zhou, Q. (2017).** *Research on teh vechicle-mounted inspection technology of tunnel lining surfaces* [master's degree, China Academy of Railway Sciences]. <https://kns.cnki.net/KCMS/detail/detail.aspx?dbname=CMFD201801&filename=1017177864.nh>
- Zhu, X., Wang, T., Liu, Y., & Huang, T. (2010).** A new defect detection technology for long-distance water conveyance tunnel. *Water Resources and Hydropower Engineering | Water Resour Hydr Eng*, *41*(12), 78-81. <https://doi.org/10.13928/j.cnki.wrahe.2010.12.013>